



Creation of MOFs with open metal sites by partial replacement of metal ions with different coordination numbers

Journal:	<i>Dalton Transactions</i>
Manuscript ID	DT-COM-10-2018-004218.R1
Article Type:	Communication
Date Submitted by the Author:	26-Nov-2018
Complete List of Authors:	<p>Harada, Yuki; Nagoya University, Department of Chemistry and Biotechnology, School of Engineering</p> <p>Hijikata, Yuh; Nagoya University, Institute of Transformative Bio-Molecules</p> <p>Kusaka, Shinpei; Nagoya University, Department of Chemistry and Biotechnology, School of Engineering</p> <p>Hori, Akihiro; Nagoya University, Department of Chemistry and Biotechnology, School of Engineering</p> <p>Ma, Yunsheng; Nagoya University, of Chemistry and Biotechnology, School of EngineeringDepartment</p> <p>Matsuda, Ryotaro; Nagoya University, Department of Chemistry and Biotechnology, School of Engineering</p>

Creation of MOFs with open metal sites by partial replacement of metal ions with different coordination numbers

Received 00th January 20xx,
Accepted 00th January 20xx

Yuki Harada,^a Yuh Hijikata,^b Shinpei Kusaka,^a Akihiro Hori,^a Yunsheng Ma,^{a,c} and Ryotaro Matsuda^{*a}

DOI: 10.1039/x0xx00000x

www.rsc.org/

Herein, we developed isostructural metal–organic frameworks (MOFs) containing open metal sites of the form $[\text{Cu}_{1-x}\text{Pd}_x(\text{SiF}_6)(\text{bpy})_2]$ (bpy: 4,4'-bipyridine) (SIFSIX-1-CuPd-3, -5 and -10) using a partial metal-replacement approach. Starting from the SIFSIX-1-Cu-type MOF, some of the Cu^{2+} ions having octahedral geometry were successfully replaced with Pd^{2+} ions having square planar geometry in different ratios while the framework structure was maintained. The results showed that gas adsorption properties of SIFSIX-1-Cu-type MOFs can be tuned via partial metal replacement.

Introducing chemically active sites into the nanopores present in porous materials is a viable strategy to increase selectivity in gas adsorption and separation materials which rely on host–guest interactions between active sites and gas molecules.¹ Open metal sites (OMSs) are a widely researched form of active sites that can recognize specific molecules, resulting in highly selective gas trapping.² Metal–organic frameworks (MOFs)³ are nanoporous materials comprising metal ions and organic ligands that present a wide variety of frameworks and pore structures. The introduction of OMSs has been applied to MOFs, resulting in the development of gas separation materials based on MOFs with OMSs.⁴ However, the incorporation of specific desirable OMSs into MOF remains a significant challenge because OMSs are reactive and are typically capped by other reactants during MOF synthesis, resulting in the saturation of the metal centres and the formation of undesired structures.

Thus, a universal methodology to incorporate OMSs into MOFs without affecting the desired frameworks is required.

To overcome these problems, we have adopted a partial metal-replacement approach to prepare MOFs with OMSs. Metal replacement is known as the useful method to modify the pore functionalities.⁵ Our strategy is that the metal ions in the original MOF are partially replaced with other metal ions having different coordination numbers, resulting in the generation of OMSs while maintaining the parent structure. Specifically, we doped Pd^{2+} ions into Cu^{2+} -based MOF $[\text{Cu}(\text{SiF}_6)(\text{bpy})_2]$ (bpy: 4,4'-bipyridine) (SIFSIX-1-Cu)⁶ (Fig. S1[†]) to obtain MOFs of the form $[\text{Cu}_{1-x}\text{Pd}_x(\text{SiF}_6)(\text{bpy})_2]$, (where $x = 0.0356, 0.0446$ and 0.0969 determined by scanning electron microscopy (SEM) for SIFSIX-1-CuPd-3, SIFSIX-1-CuPd-5 and SIFSIX-1-CuPd-10, respectively).

The partial exchange of Cu^{2+} , which has octahedral geometry, with Pd^{2+} , which has square planar geometry, changes the coordination number of the metal ion sites and introduces OMSs (Fig. 1) while maintaining the original structure and its stability.

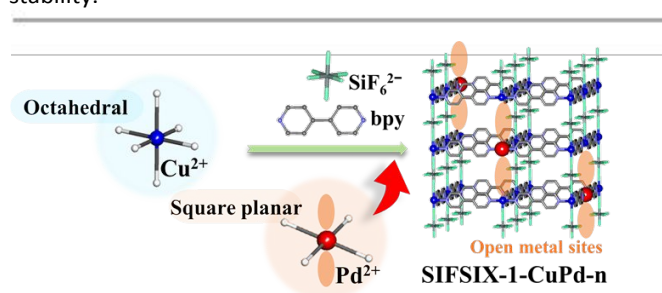


Fig. 1 Schematic illustration of SIFSIX-1-CuPd-n formation.

Bulk SIFSIX-1-CuPd-n powders were synthesized by heating an $\text{H}_2\text{O}/\text{EtOH}$ solution of $\text{Cu}(\text{BF}_4)_2 \cdot 6\text{H}_2\text{O}$ (20 mM), $(\text{NH}_4)_2\text{SiF}_6$ (20 mM), bpy (40 mM) and different amounts of $\text{Pd}(\text{en})(\text{ONO}_2)_2$ (en: ethylenediamine), for 3 h at 100 °C under microwave irradiation. The resulting purple crystals were collected and activated at 120 °C under vacuum for 24 h.

^a Department of Chemistry and Biotechnology, School of engineering, Nagoya University, Chikusa-ku, Nagoya 464-8603, Japan.

E-mail: ryotaro.matsuda@chembio.nagoya-u.ac.jp

^b Department of Chemistry, Graduate School of Science and Institute of Transformative Bio-Molecules (WPI-ITbM), Nagoya University, Chikusa-ku, Nagoya 464-8602, Japan.

^c School of Chemistry and Materials Engineering, Jiangsu Key Laboratory of Advanced Functional Materials, Changshu Institute of Technology, Changshu, Jiangsu 215500, PR China.

[†] Electronic Supplementary Information (ESI) available: Synthetic methods, characterization data, TG data, sorption data, and calculation data.

DOI: 10.1039/x0xx00000x

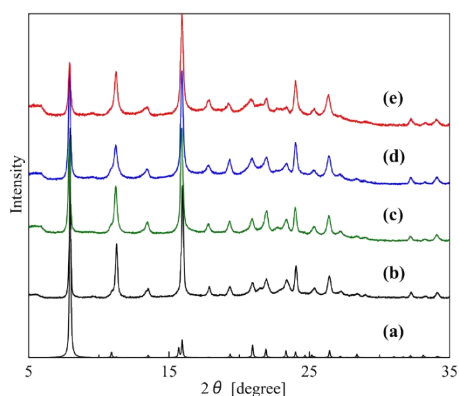


Fig. 2 PXRD patterns of (a) simulated **SIFSIX-1-Cu**, and as-synthesized (b) **SIFSIX-1-Cu**, (c) **SIFSIX-1-CuPd-3**, (d) **SIFSIX-1-CuPd-5** and (e) **SIFSIX-1-CuPd-10**.

The obtained powder X-ray diffraction (PXRD) patterns of **SIFSIX-1-CuPd-n** were in good agreement with the simulated patterns of **SIFSIX-1-Cu**, confirming that **SIFSIX-1-Cu** and **SIFSIX-1-CuPd-n** are isostructural (Fig. 2). No peak due to Pd metal was observed at 40.02° (Fig. S2[†]).⁷ These structures were stable under atmospheric condition for eight months, which were confirmed by PXRD patterns (Fig. S3[†]). The results showed that these compounds have enough chemical stability to handle without any special care or treatment. The Fourier-transform infrared (FT-IR) spectra of **SIFSIX-1-CuPd-n** (Fig. S4[†]) were almost identical. In addition, no peaks derived from NO_3^- (1380 cm^{-1}) or ethylenediamine (1170 cm^{-1}) were observed (Fig. S5[†]). These results demonstrate the phase purity of the **SIFSIX-1-CuPd-n** samples. To obtain more detailed structural information, SEM, scanning transmission electron microscopy (STEM) and energy dispersive X-ray analysis (EDX) were performed. No Cu or Pd nanoparticles were observed in either the SEM (Fig. S6[†]) or STEM images (Fig. S7[†]). EDX mapping (Fig. S6, S7[†]) revealed that Cu^{2+} and Pd^{2+} were uniformly dispersed throughout the crystals. Furthermore, the $\text{Pd}^{2+}/\text{Cu}^{2+}$ ratios were close to those adopted in the preparation of **SIFSIX-1-CuPd-n** (Table S1, S2[†]). These results demonstrate that the partial replacement of Cu^{2+} in **SIFSIX-1-Cu** with Pd^{2+} was successful.

Fig. 3 and S8[†] show the X-ray photoelectron spectroscopy (XPS) analysis of Cu and Pd in **SIFSIX-1-CuPd-10**. The spectra exhibit double peaks at binding energies of 337.4 and 342.6 eV, corresponding to the two Pd doublet peaks ($3d_{5/2}$ and $3d_{3/2}$), respectively. These binding energies are typical of square planar four-coordinated Pd^{2+} , indicating that no Pd^0 , Pd^{3+} or Pd^{4+} species exist inside the framework. Furthermore, the four Cu peaks indicate the presence of two types of Cu^{2+} . Two of the peaks are derived from Cu^{2+} ions neighboring another Cu^{2+} ion, whereas the other two peaks are derived from Cu^{2+} ions neighboring a Pd^{2+} ion.

The thermogravimetric analysis curves for **SIFSIX-1-CuPd-n** show weight loss derived from framework decomposition at $\sim 180^\circ\text{C}$, which is close to the corresponding value for **SIFSIX-1-Cu** (200°C), demonstrating that these new MOFs have similar structural stability to the parent structure **SIFSIX-1-Cu** (Fig. S9[†]).

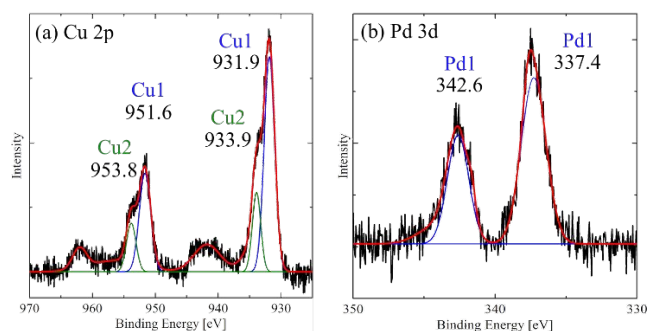


Fig. 3 XPS spectrum of **SIFSIX-1-CuPd-10**. (a) Cu peaks: two peaks (962 eV and 942 eV) are Cu^{2+} satellite peaks. (b) Pd peaks.

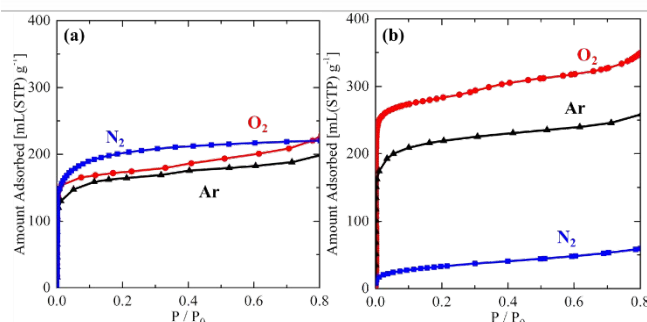


Fig. 4 Adsorption isotherms of O_2 , N_2 and Ar at 77 K for (a) **SIFSIX-1-Cu** and (b) **SIFSIX-1-CuPd-10**.

To demonstrate the functionality of **SIFSIX-1-CuPd-n** MOFs, we evaluated their gas adsorption properties. Fig. 4 and S10[†] show the adsorption isotherms for **SIFSIX-1-Cu** and **SIFSIX-1-CuPd-10**. The saturated adsorption amounts of N_2 , O_2 and Ar for **SIFSIX-1-Cu** for $P/P_0 < 0.8$ were almost identical (ca. 200 mL/g). On the other hand, those for **SIFSIX-1-CuPd-10** for $P/P_0 < 0.8$ were quite different (N_2 : ca. 60 mL/g, O_2 : ca. 350 mL/g, Ar: ca. 260 mL/g). The adsorption amount of O_2 for **SIFSIX-1-CuPd-10** at $P/P_0 < 0.8$ was much larger than that for **SIFSIX-1-Cu** whereas the adsorption amounts of Ar for both compounds are identical. This suggests that introduced Pd-OMSs interact with O_2 more strongly than Ar. Moreover, adsorption isotherms of O_2 for **SIFSIX-1-CuPd-n** ($n = 3, 5, 10$) (Fig. S11[†]) showed that as the ratio of Pd^{2+} increased, the amount of O_2 adsorption also increased under the low pressure, while the effect was small on Ar adsorption (Fig. S12[†]). These results also support that Pd-OMSs enhanced the O_2 adsorption. On the other hand, amount of N_2 adsorption significantly decreased as the ratio of Pd^{2+} increased (Fig. S13[†]). As Pd^{2+} is usually four-coordinate, SiF_6^{2-} counter anions would be contained in the pores rather than acting as pillar ligands. This SiF_6^{2-} hinders gas diffusion, preventing N_2 molecules from completely entering the pores due to the large molecular size of N_2 (3.64 \AA), while such effect might be much smaller for O_2 (3.46 \AA) and Ar (3.4 \AA) than N_2 .⁸

To investigate the effect of the OMSs on the adsorption behaviour of the proposed MOFs, density functional theory calculations were performed with the M06 functional using Gaussian 09. The SDD basis set⁹ was employed for Pd^{2+} where the core electrons were replaced with the effective core

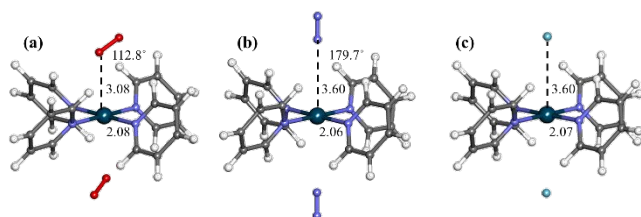


Fig. 5 The optimized structures of (a) $\text{Pd}(\text{py})_4\text{-O}_2$ (b) $\text{Pd}(\text{py})_4\text{-N}_2$ and (c) $\text{Pd}(\text{py})_4\text{-Ar}$.

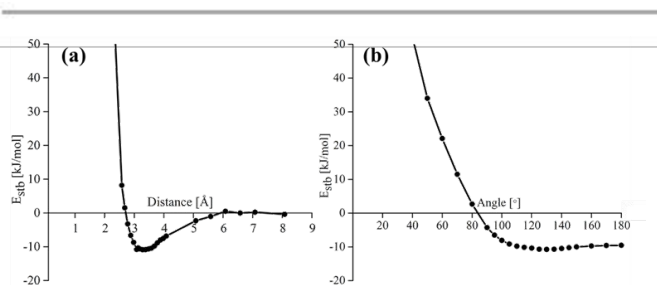


Fig. 6 The E_{stb} depending on the (a) Pd-O distance and (b) Pd-O-O angle.

potential, and the cc-pVTZ basis set¹⁰ was employed for others. A model of the OMS unit was constructed using Pd^{2+} and four pyridine molecules (py) which coordinated to the central Pd^{2+} i.e. $\text{Pd}(\text{py})_4$ (Fig. S14[†]). After optimizing the geometry of $\text{Pd}(\text{py})_4$ with O_2 , N_2 and Ar molecules located at the axial positions ($\text{Pd}(\text{py})_4\text{-X}$, X = O_2 , N_2 or Ar), the structures were re-optimised (Fig. 5). The stabilisation energy (E_{stb}) is defined using the following equation with counterpoise corrections:

$$E_{\text{stb}} = \frac{1}{2} \{ E_{\text{complex}} - (E_{\text{Pd}(\text{py})_4} + 2E_{\text{X}}) \}$$

where E_{complex} , $E_{\text{Pd}(\text{py})_4}$ and E_{X} are the single point energies at the optimised geometry for $\text{Pd}(\text{py})_4\text{-X}$, $\text{Pd}(\text{py})_4$ and X, respectively. The obtained E_{stb} values are -15.4 kJ/mol, -14.8 kJ/mol and -13.1 kJ/mol where X are O_2 , N_2 and Ar, respectively, indicating that O_2 interacts with the frameworks more favourably than N_2 and Ar. This demonstrates that the Pd^{2+} centres act as OMSs, which may influence the adsorption mechanism. In addition, we evaluated the dependence of E_{stb} on the Pd-O distance and Pd-O-O angle. The calculated potential curves are shown in Fig. 6. The energy-minimised geometry featured a Pd-O distance of 3.08 Å and a Pd-O-O angle of 112.8° . This is in contrast to the case of N_2 , wherein the distances of Pd-N and Pd-Ar were both 3.60 Å, and the Pd-N-N angle was 179.7° . The difference in the structure also suggests the favourable interaction of O_2 with Pd^{2+} centres over those of N_2 and Ar.

In conclusion, we have developed a new methodology to incorporate OMSs into MOFs using a partial metal-replacement approach. The replacement of Cu^{2+} ions having octahedral geometry with Pd^{2+} ions having square planar geometry effectively forms OMSs in the mother structure while maintaining the topology of the initial framework. The adsorption behaviour of the MOFs was tuned by the incorporation of the OMSs which provided different interactions with different gas molecules. The findings of this study will pave the way towards novel highly functionalised MOFs with OMSs.

Conflicts of interest

There are no conflicts of interest to declare.

Acknowledgements

This work was supported by the PRESTO (Grant No. JPMJPR141C), ACCEL project (Grant No. JPMJAC1302) and CREST (Grant No. JPMJCR1713) of the Japan Science and Technology Agency (JST), and JSPS KAKENHI Grant-in-Aid for Young Scientists (A) (Grant No.16H06032).

Notes and references

- (a) Z. Zhang, Y. Zhao, Q. Gong, Z. Li, J. Li, *Chem. Commun.*, 2013, **49**, 653–661; (b) V. M. Suresh, S. Bonakala, H. S. Atreya, S. Balasubramanian, T. K. Maji, *ACS Appl. Mater. Interfaces*, 2014, **6**, 4630–4637; (c) R. W. Flaig, T. M. O. Popp, A. M. Fracaroli, E. A. Kapustin, M. J. Kalmutzki, R. M. Altamimi, F. Fathieh, J. A. Reimer, O. M. Yaghi, *J. Am. Chem. Soc.*, 2017, **139**, 12125–12128; (d) H. Sato, R. Matsuda, K. Sugimoto, M. Takata, S. Kitagawa, *Nat. Mater.*, 2010, **9**, 661–666.
- (a) H. R. Moon, N. Kobayashi, M. P. Suh, *Inorg. Chem.*, 2006, **45**, 8672–8676; (b) H. Wu, W. Zhou, T. Yildirim, *J. Am. Chem. Soc.*, 2009, **131**, 4995–5000; (c) Z. Guo, H. Wu, G. Srinivas, Y. Zhou, S. Xiang, Z. Chen, Y. Yang, W. Zhou, M. O’Keeffe, B. Chen, *Angew. Chem. Int. Ed.*, 2011, **50**, 3178–3181.
- (a) M. Eddaoudi, J. Kim, M. Rosi, D. Vodak, J. Wachter, M. O’Keeffe, O. M. Yaghi, *Science*, 2002, **295**, 469–472; (b) S. Kitagawa, R. Matsuda, *Coord. Chem. Rev.*, 2007, **251**, 2490–2509; (c) G. Férey, C. Serre, *Chem. Soc. Rev.*, 2009, **38**, 1380–1399.
- (a) P. D. C. Dietzel, V. Besikiotis, R. Blom, *J. Mater. Chem.*, 2009, **19**, 7362–7370; (b) Y. Bae, C. Y. Lee, K. C. Kim, O. K. Farha, P. Nickias, J. T. Hupp, S. T. Nguyen, R. Q. Snurr, *Angew. Chem. Int. Ed.*, 2012, **51**, 1857–1860; (c) E. D. Bloch, W. L. Queen, R. Krishna, J. M. Zadrozny, C. M. Brown, J. R. Long, *Science*, 2012, **335**, 1606–1610; (d) H. Sato, W. Kosaka, R. Matsuda, A. Hori, Y. Hijikata, R. V. Belosludov, S. Sakaki, M. Takata, S. Kitagawa, *Science*, 2014, **343**, 167–170; (e) A. Mallick, S. Saha, P. Pachfule, S. Roy, R. Banerjee, *J. Mater. Chem.*, 2010, **20**, 9073–9080; (f) B. Garai, A. Mallick, A. Das, R. Mukherjee, R. Banerjee, *Chem. Eur. J.*, 2017, **23**, 7361–7366.
- (a) D. Denysenko, T. Werner, M. Grzywa, A. Puls, V. Hagen, G. Eickerling, J. Jelic, K. Reuter, D. Volkmer, *Chem. Commun.*, 2012, **48**, 1236–1238; (b) M. Kim, J. F. Cahill, H. Fei, K. A. Prather, S. M. Cohen, *J. Am. Chem. Soc.*, 2012, **134**, 18082–18088; (c) D. Sun, F. Sun, X. Deng, Z. Li, *Inorg. Chem.*, 2015, **54**, 8639–8643; (d) W. Zhang, Z. Chen, M. Al-Naji, P. Guo, S. Cwik, O. Halbherr, Y. Wang, M. Muhler, N. Wilde, R. Glaser, R. A. Fischer, *Dalton. Trans.*, 2016, **45**, 14883–14887.
- (a) S. Subramanian, M. J. Zaworotko, *Angew. Chem. Int. Ed. Engl.*, 1995, **34**, 2127–2129; (b) S. Noro, S. Kitagawa, M. Kondo, K. Seki, *Angew. Chem. Int. Ed.*, 2000, **39**, 2081–2084; (c) X. Cui, K. Chen, H. Xing, Q. Yang, R. Krishna, Z. Bao, H. Wu, W. Zhou, X. Dong, Y. Han, B. Li, Q. Ren, M. J. Zaworotko, B. Chen, *Science*, 2016, **353**, 141–144.
- M. Khan, M. Khan, M. Kuniyil, S. F. Adil, A. Al-Warthan, H. Z. Alkhatlan, W. Tremel, M. N. Tahir, M. R. H. Siddiqui, *Dalton. Trans.*, 2014, **43**, 9026–9031.
- D. W. Breck, *Zeolite molecular sieves: structure, chemistry, and use*, Wiley, New York, 1973.
- X. Y. Cao and M. Dolg, *Theochem. J. Mol. Struct.*, 2002, **581**, 59–139.

COMMUNICATION

Journal Name

- 10 A. Wilson, T. V. Mourik, T. H. Dunning Jr., *Theochem. J. Mol. Struct.*, 1997, **388**, 339.